[3] Miller, W. H., "Experimentally Measured Bond Stresses in a Full-Scale Motor," AIAA Paper 68-510, Atlantic City, N. J., 1968.

[4] Cost, T. L., "Analytical Methods for Determining the Shrinkage Stresses in Polymeric Materials During Cure," TR S-72, Dec. 1968, Rohm and Haas Co., Redstone Research Labs.

High-Fidelity Solar Simulation for an Ultrahigh Vacuum Facility

DEWEY E. WORNOM*
NASA Langley Research Center, Hampton, Va.
AND
F. N. BENNING†
Spectrolab Division of Textron Industries, Sylmar, Calif.

SOLAR simulation has been provided for the Langley Research Center 150-ft[3] Space Vacuum Facility. The facility vacuum chamber, 7½ ft in diameter and 12 ft long, is shown in Fig. 1. The concentric cylindrical walls of the chamber consist of a conventional outer wall, a liquid-nitrogen-cooled inner wall, and an innermost liquid-helium-cooled cryopanel enclosing a 150-ft[3] test volume. The volume within the inner chamber wall is pumped by a main oil diffusion pumping system while a guard volume, between the inner and outer chamber walls, is differentially pumped by a separate oil diffusion pumping system. Access to the test volume is provided by a full-diameter hinged door on the outer wall and removable cylindrical doors on the inner wall and cryopanel. From standard atmospheric conditions, the chamber is capable of obtaining ultimate pressures below 10^{-10} torr within 24 hr. Complete details of the facility and its performance capabilities are given in Refs. 1 and 2.

Chamber Modification for Solar Simulation

The criterion for modifying the chamber for solar simulation was to introduce any additional gas load to the guard volume rather than to the test volume, avoid creating a direct leak from outside the chamber into the test volume, and allow return of the chamber to its original configuration and performance capability when solar simulation was not required. This criterion was satisfied by use of an on-axis type simulator that permitted, as shown in Fig. 2, simple and direct penetration through the chamber doors. Therefore, chamber modification consisted of replacing the chamber doors with new doors having openings approximately 3 ft in diam. Upon coupling the simulator to the outer chamber door, the cylindrical end of the transition cone compresses the metal bellows attached to the inner chamber door opening and the simulator collimating lens becomes the vacuum closure for the opening. And, through ports in the cylindrical end of the cone, the cone volume becomes part of the chamber guard volume with the simulator tipping lens acting as the vacuum closure for the cone. The use of simulator optical elements instead of flat windows as vacuum closures for the door penetrations avoided the unnecessary degradation of the simulator beam that windows would have created.

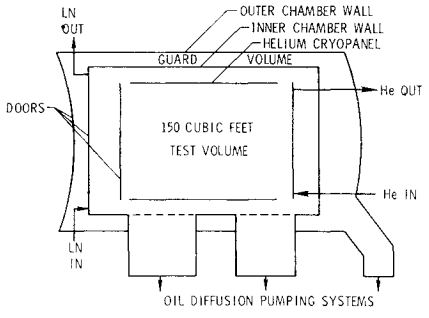

Fig. 1 150-ft[3] space vacuum facility.

Solar Simulator Design

The major components of the simulator system, noted in Fig. 2, consist of thirteen 2.5-kw xenon energy sources, collectors, folding mirrors, field lens assembly, and projection lens assembly, all enclosed within a sealed radiation housing. This housing is continuously purged with cold gaseous nitrogen which acts as a coolant and eliminates formation of ozone. The remaining optical elements, a tipping and a collimating lens, are held within the transition cone that couples the radiation housing to the chamber.

Power for the multiple energy sources is provided by individual power supplies filtered for a d.c. current ripple of less than 1%. System operation is initiated by energizing the energy sources then regulating their current individually or collectively to obtain the selected beam intensity level. Thereafter, the selected intensity is automatically maintained by a light-sensored (sensors located near each source) closed-loop control system. The complete system is operated and monitored from a central control console where annunciation of any cooling or electrical subsystem malfunction is also indicated.

Energy from each source is intercepted then reflected by their collectors onto the first folding mirror. The combined energy of each energy source is then redirected by the folding mirrors into the field lens assembly. This lens assembly, consisting of seven small lenses clustered side by side, separates the circular beam into seven circular light channels. Seven corresponding small lenses in the projection lens assembly intercept and magnify each light channel to fill the collimating lens. Since six of the seven light channels are off of the optical axis, the tipping lens tips these channels to coincide with the collimating lens. The combining of each light channel onto the collimating lens, as well as the energy from each energy source onto the first folding mirror, is for the purpose of improving the uniformity of the beam across its diameter. And, finally, the 36-in.-diam collimating lens provides a 27-in.-diam collimated beam within the chamber test volume.

Also included in the optical system, but not noted in Fig. 2, is a manually operated beam douser that permits beam interruption without de-energizing the energy sources, a beam adjuster that allows adjustment of beam size and shape, and a spectral filter that removes most of the beam spectral content outside of the natural solar spectrum.

Table 1 Solar simulator performance

Simulator characteristics	Test results
Intensity range:	½ to 2 s.c.
Uniformity:	
At ½ s.c.	±6.6%
2 s.c.	±5.6%
Collimation angle:	±3°
Spectral match:	See Table 2
Beam stabilization:	In 12 min
Auto. intensity control:	<1%

Presented as Paper 69-1001 at the AIAA/ASTM/IES 4th Space Simulation Conference, Los Angeles, Calif., September 8–10, 1969; submitted September 29, 1969; revision received November 10, 1969.

* Aerospace Technologist, Applied Materials and Physics Division. Associate Fellow AIAA.

† Technical Director, System Division. Member AIAA.

Performance of the Solar Simulator

Simulator beam characteristics were measured with the simulator completely assembled optically but not coupled to the chamber.

The results of simulator performance measurements are presented in Tables 1 and 2. Total intensity range was determined by a calibrated radiometer. Three to 10 lamps were used for the specified total intensity range. Lower or higher intensities than those specified in Table 1 can be obtained since one to 13 lamps can be operated. Rotational uniformity scans, at one-half and two solar constants (sc) were made at three locations along the length of the beam within the chamber test volume. Measurements, in incremental radii of 3 in., were made with a 4- by 4-cm array of solar cells. Collimation angle was determined from the geometrical relationship between the image source size and the distance between the image and the decollimation pinhole point.

A total of 11 spectral measurements were made, for both 0.5 sc and 2 sc, throughout the portion of the beam within the chamber test volume. (The measurements were taken at 11 locations within the beam. At each location the measurements were broken down in 14 bandwidths as noted in Fig. 2.) The range of deviation from the NRL (Naval Research Laboratory) solar distribution curve of the 11 measurements taken for each bandwidth and intensity level is listed in Table 2. The measurements were made by a double prism monochromator calibrated with a 1000-w NBS (National Bureau of Standards) Standard of Spectral Irradiance. A photomultiplier detector was employed for wavelengths from 0.25 to 0.65 μ and a lead sulfide detector for wavelengths from 0.45 to 2.7 μ. Radiation from both the standard lamp and solar simulator was diffused by a quartz transmissive diffuser prior to passing through the monochromator entrance slit.

A 24-hr continuous unattended operational test was performed on the system in which its ability to stabilize and automatically maintain a preset total intensity level was determined. Beam intensity stabilization and total intensity variations were measured by a solar cell whose output was recorded on a chart recorder.

Chamber Performance

Chamber tests were conducted immediately before and after modifications to determine to what degree chamber performance was affected by the addition of solar simulation. Tests were conducted with the facility operated in two different modes. In one, the inner chamber was cooled down to 88°K with no flow in the helium cryopanel. In the other, the helium cryopanel was cooled down to 5°K. Pressure measurements were made with a hot cathode ionization gage calibrated for nitorgen. For the first mode, the ultimate pressure increased from 4×10^{-10} torr to 3×10^{-9} torr due to chamber modifications for solar simulation. For the second mode, the ultimate pressure reached the ionization gage x-ray limit of 3×10^{-10} torr both before and after modifications.

Table 2 Spectral match

Bandwidth, μ	Deviation from NRL curve, %	
	2 s.c.	$\frac{1}{2}$ s.c.
0.25 to 0.33	−25.1 to 47.7	−12.1 to −51.8
0.33 to 0.40	9.0 to −10.2	20.4 to 3.0
0.40 to 0.50	0.7 to −11.0	5.4 to −1.9
0.50 to 0.60	1.8 to −2.3	6.1 to −0.3
0.60 to 0.70	−0.1 to −2.6	2.7 to −3.6
0.70 to 0.80	8.9 to −4.4	0.1 to −6.9
0.80 to 0.90	5.6 to −14.6	0.5 to −22.5
0.90 to 1.00	1.5 to −11.5	3.3 to −21.1
1.00 to 1.20	7.9 to 1.0	9.4 to −5.6
1.20 to 1.40	−11.3 to −17.0	−13.9 to −20.8
1.40 to 1.60	53.6 to 39.2	46.2 to 28.9
1.60 to 2.00	25.5 to 9.8	14.9 to −2.1
2.00 to 2.40	38.6 to −15.6	26.6 to −0.7
2.40 to 2.70	−12.4 to −30.9	15.5 to −43.0

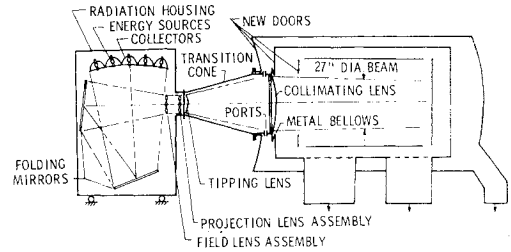

Fig. 2 Combined solar-vacuum facility.

References

[1] Elderkin, C. D. and Bradford, J. M., "A Large Ultra High Vacuum Environmental Chamber With Liquid Helium Cooled Walls," paper presented at 1965 Institute of Environmental Sciences Symposium, April 1965.

[2] Gregory, G. L., Bradford, J. M., and Mugler, J. P., Jr., "Vacuum Capabilities of the 150-Cubic-Foot Space Vacuum Facility at the Langley Research Center," *AIAA/IES/ASTM Space Simulation Conference*, AIAA, New York, 1966.

Radiation Interchange Interior to Multilayer Insulation Blankets

R. K. MacGregor,* J. T. Pogson,* and D. J. Russell†
The Boeing Company, Aerospace Systems Division, Seattle, Wash.

MULTILAYER insulation blankets provide a lightweight insulation system with a high thermal resistance. The multilayer blankets consist of a number of highly reflecting radiation shields interspaced with a low thermal conductivity spacer material or separated by crinkling the radiation shields themselves. The radiation shields are generally mylar or kapton films metalized on one or both sides. Spacer materials range from very coarse silk or nylon net to continuous materials such as a borosilicate fiber glass paper.‡ While heat transfer through the insulation normal to the layers is small, there are large energy losses at seams and

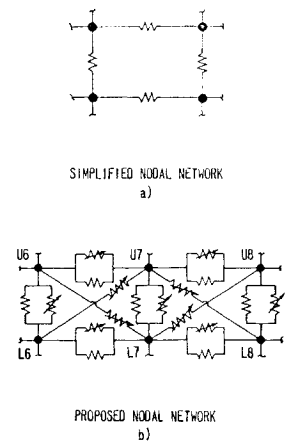

Fig. 1 Nodal networks utilized for multilayer insulation calculations.

Received October 20, 1969.
* Research Specialist. Member AIAA.
† Research Engineer
‡ Tissue glass.